Differential mechanisms of Cantú syndrome–associated gain of function mutations in the *ABCC9* (SUR2) subunit of the K_{ATP} channel

Paige E. Cooper,[1,2]* Monica Sala-Rabanal,[1,2]* Sun Joo Lee,[1,2] and Colin G. Nichols[1,2]

[1]Department of Cell Biology and Physiology, and [2]Center for the Investigation of Membrane Excitability Diseases, Washington University School of Medicine, Saint Louis, MO 63110

Cantú syndrome (CS) is a rare disease characterized by congenital hypertrichosis, distinct facial features, osteochondrodysplasia, and cardiac defects. Recent genetic analysis has revealed that the majority of CS patients carry a missense mutation in *ABCC9*, which codes for the sulfonylurea receptor SUR2. SUR2 subunits couple with Kir6.x, inwardly rectifying potassium pore-forming subunits, to form adenosine triphosphate (ATP)-sensitive potassium (K_{ATP}) channels, which link cell metabolism to membrane excitability in a variety of tissues including vascular smooth muscle, skeletal muscle, and the heart. The functional consequences of multiple uncharacterized CS mutations remain unclear. Here, we have focused on determining the functional consequences of three documented human CS-associated *ABCC9* mutations: human P432L, A478V, and C1043Y. The mutations were engineered in the equivalent position in rat SUR2A (P429L, A475V, and C1039Y), and each was coexpressed with mouse Kir6.2. Using macroscopic rubidium ($^{86}Rb^{+}$) efflux assays, we show that K_{ATP} channels formed with P429L, A475V, or C1039Y mutants enhance K_{ATP} activity compared with wild-type (WT) channels. We used inside-out patch-clamp electrophysiology to measure channel sensitivity to ATP inhibition and to MgADP activation. For P429L and A475V mutants, sensitivity to ATP inhibition was comparable to WT channels, but activation by MgADP was significantly greater. C1039Y-dependent channels were significantly less sensitive to inhibition by ATP or by glibenclamide, but MgADP activation was comparable to WT. The results indicate that these three CS mutations all lead to overactive K_{ATP} channels, but at least two mechanisms underlie the observed gain of function: decreased ATP inhibition and enhanced MgADP activation.

INTRODUCTION

ATP-sensitive potassium (K_{ATP}) channels, found in many excitable tissues, including brain (Ashford et al., 1988), heart (Noma, 1983), pancreatic islets (Cook and Hales, 1984), and skeletal and smooth muscle (Standen et al., 1989; Winquist et al., 1989) are hetero-octameric protein complexes composed of four pore-forming inwardly rectifying potassium channel Kir6.X subunits, each associated with one sulfonylurea receptor subunit (SURX) (Shyng and Nichols, 1997). K_{ATP} channels link cell metabolism with membrane excitability as a result of intracellular nucleotide regulation of channel activity. ATP binds directly to the pore-forming Kir6.X subunits (Tucker et al., 1997) to inhibit the channel, and MgADP binds to SURX to activate the channel (Nichols et al., 1996). Channels formed from different combinations of Kir6.1 (*KCNJ8*), Kir6.2 (*KCNJ11*) (Inagaki et al., 1995a,b), SUR1 (*ABCC8*), and SUR2 (*ABCC9*) subunit isoforms vary in nucleotide sensitivity and pharmacology (Masia et al., 2005), as well as tissue localization (Aguilar-Bryan et al., 1995; Inagaki et al., 1996), generating additional functional diversity of K_{ATP} channels (Nichols, 2006; Akrouh et al., 2009).

Cantú syndrome (CS) was first recognized as a unique disorder in 1982 (Cantú et al., 1982). Clinical hallmarks of CS include hypertrichosis, macrosomia, macrocephaly, coarse facial appearance, cardiomegaly, and skeletal abnormalities (Harakalova et al., 2012; van Bon et al., 2012; Cooper et al., 2014). Recent studies have shown that the majority of known CS patients have missense mutations in *ABCC9* (Harakalova et al., 2012; van Bon et al., 2012) or *KCNJ8* (Brownstein et al., 2013; Cooper et al., 2014) that result in a gain of function (GOF) in K_{ATP} channel activity. CS resulting from mutations in either subunit confirms that functional changes in the K_{ATP} channels formed from them underlie the disease.

Conversely, *KCNJ11* and *ABCC8*, which encode Kir6.2 and SUR1, respectively, generate K_{ATP} channels in pancreatic β cells (Inagaki et al., 1995a), and GOF mutations in either of these subunits give rise to neonatal diabetes mellitus (NDM) (Gloyn et al., 2004; Babenko et al., 2006), characterized by decreased insulin secretion and elevated blood glucose levels. Detailed analyses of NDM

*P.E. Cooper and M. Sala-Rabanal contributed equally to this paper.
Correspondence to Colin G. Nichols: cnichols@wustl.edu

Abbreviations used in this paper: CS, Cantú syndrome; GOF, gain of function; K_{ATP}, ATP-sensitive potassium; MI, metabolic inhibition; NDM, neonatal diabetes mellitus; PIN, pinacidil; PIP_2, phosphatidylinositol (4,5)-bisphosphate; P_o, open probability.

The Rockefeller University Press $30.00
J. Gen. Physiol. Vol. 146 No. 6 527–540
www.jgp.org/cgi/doi/10.1085/jgp.201511495

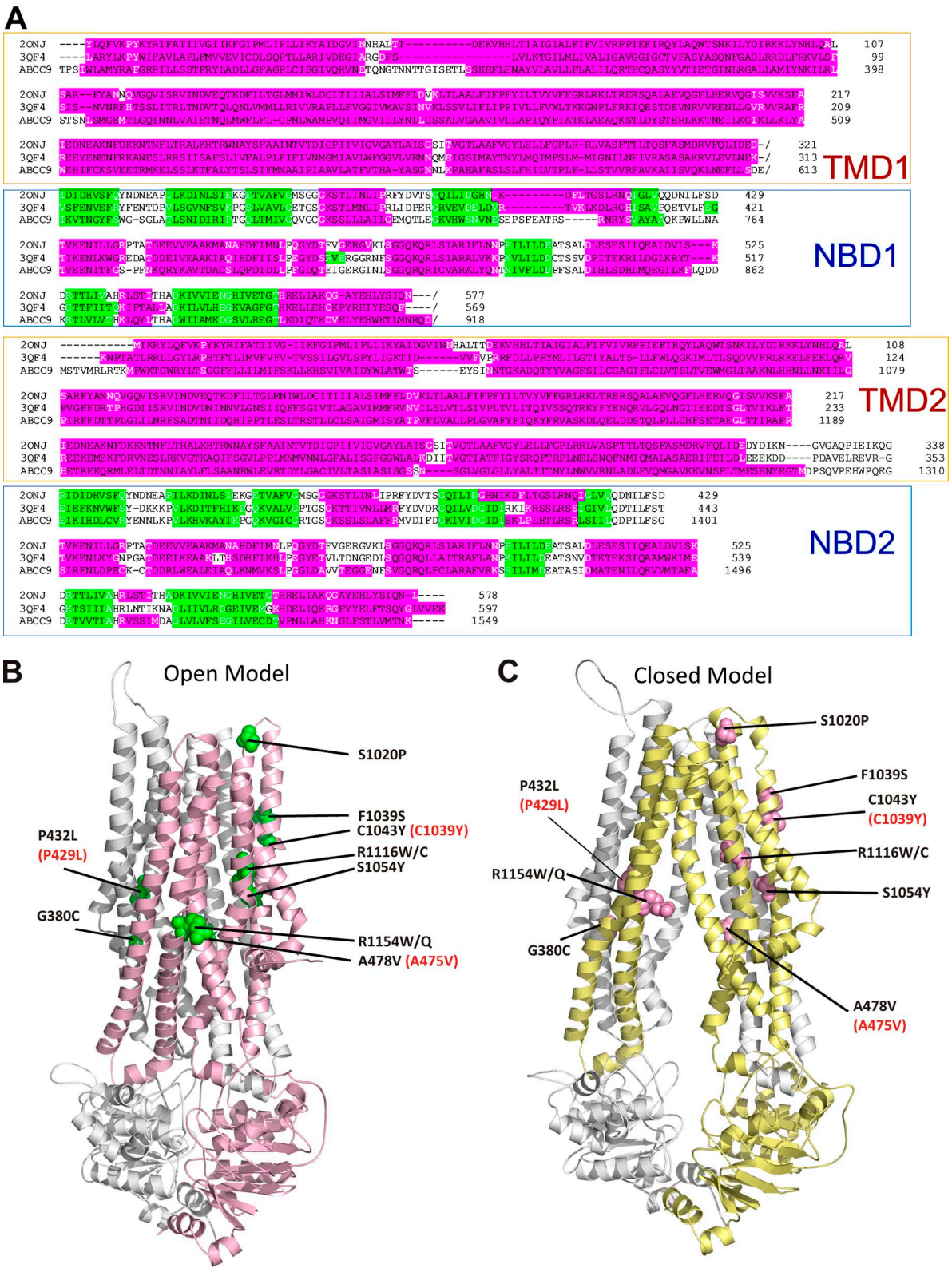

Figure 1. CS mutations in SUR2. (A) Alignment of SUR2 (ABCC9) with the multidrug ABC transporter Sav1866 (2ONJ) and heterodimeric ABC transporter TM287-TM288 (3QF4), upon which we built homology models. (B and C) Key structural domains TMD1 and 2 and NBD1 and 2 are indicated, as well as predicted α-helical (pink) and β-strand (green) segments. (B) Homology models of "open" and "closed" conformations of the SUR2A protein, which are based on *Staphylococcus aureus* Sav1866, a bacterial homologue of the human ABC transporter Mdr1 and heterodimeric ABC transporter TM287-TM288 (TM287/288) from *Thermotoga maritime*, respectively. Published CS mutations from previous reports are shown in green (open) and light pink (closed).

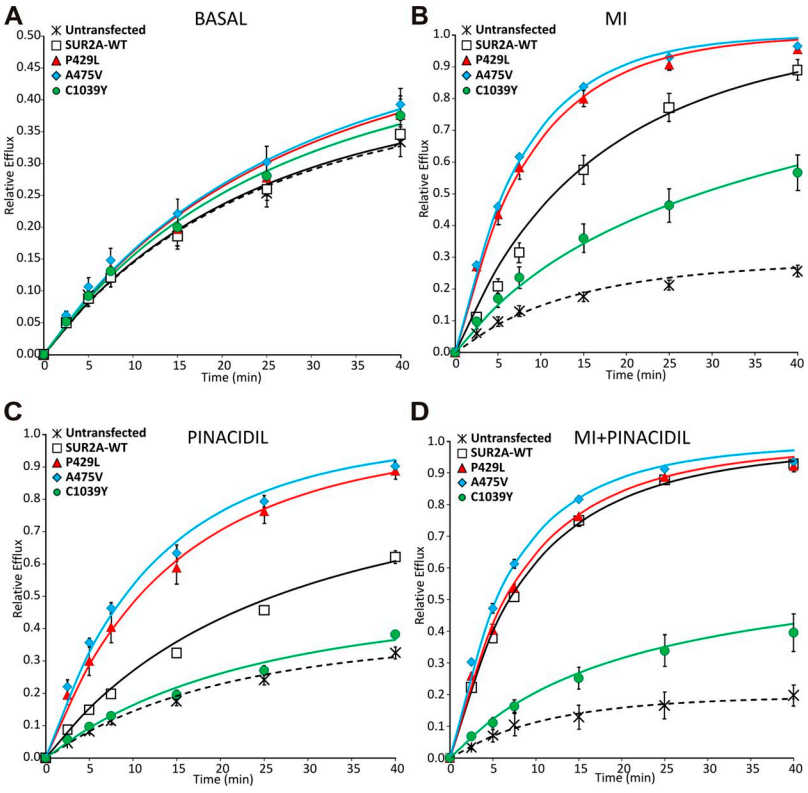

Figure 2. Increased channel activity in intact cells expressing homomeric P429L-, A475V-, or C1039Y-containing K_{ATP} channels. $^{86}Rb^+$ efflux as a function of time was measured in GFP-transfected control cells (dashed) and in cells transiently expressing reconstituted Kir6.2-based K_{ATP} channels with WT, P429L, A475V, or C1039Y SUR2 subunits in homomeric configuration, in basal conditions (A), in the presence of MIs oligomycin and 2-deoxy-D-glucose (B), in the K^+ channel opener PIN (C), or in the presence of both MI and PIN (D). The data represent means ± SEM of 6–10 experiments. Flux data were fit with Eq. 1 (GFP) to obtain the rate constant k_1 or Eq. 2 to obtain the rate constants for K_{ATP}-dependent efflux, k_2 (Fig. 3), where lines show mean fitted relationships.

mutations in *ABCC8* demonstrate that distinct molecular mechanisms can underlie the increase in channel activity, including increased open probability (P_o) (Koster et al., 2005; Babenko et al., 2006; Proks et al., 2007) and increased MgADP activation (de Wet et al., 2007b; Masia et al., 2007). To understand the molecular mechanisms

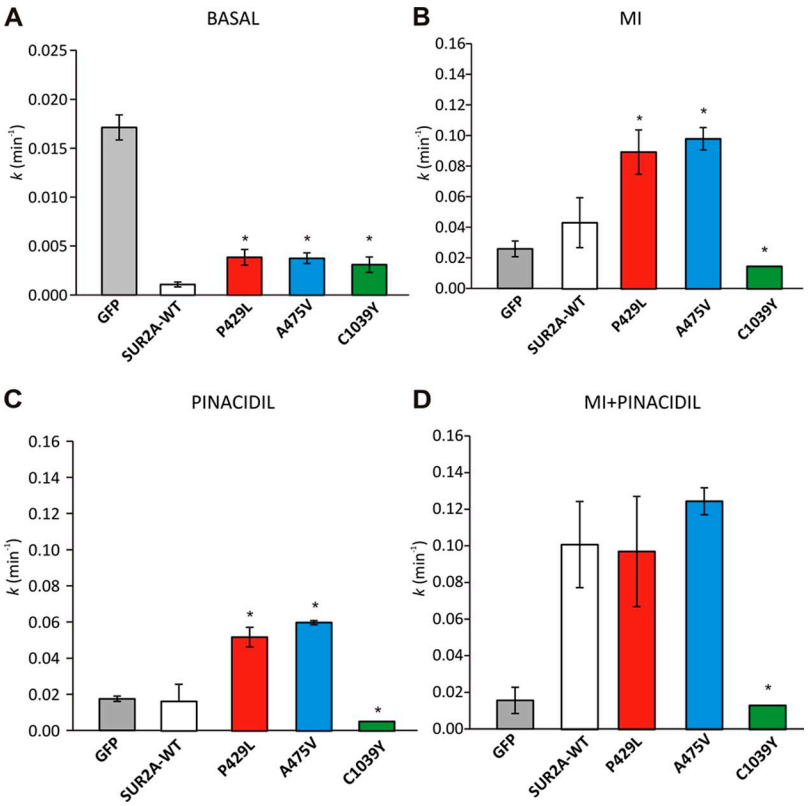

Figure 3. K_{ATP} conductance is increased in basal and stimulated conditions in intact cells expressing homomeric P429L and A475V-based K_{ATP} channels. (A–D) Rate constants for K_{ATP}-dependent $^{86}Rb^+$ efflux (k_1 in gray, proportional to nonspecific K^+ conductance and k_2, proportional to K_{ATP}-specific K^+ conductance) were calculated from data shown in Fig. 2. *, $P < 0.05$ as compared with WT (unpaired Student's *t* test). Error bars represent mean ± SEM.

of CS-associated *ABCC9* mutations, we have engineered and analyzed channel properties for three CS mutations that localize to different regions of the protein: P429L, A475V, and C1039Y. Given the experimental difficulty of recording Kir6.1/SUR2 currents (Cooper et al., 2014), we studied Kir6.2+SUR2A channels in the present experiments, and by means of $^{86}Rb^+$ efflux assays in intact cells transiently transfected with WT or mutant subunits, we confirm that all three mutations result in overactive K_{ATP} channels. Consistent with the diversity of mechanisms found in NDM patients with *ABCC8* mutations, we further show that CS-associated *ABCC9* GOF mutations can result from at least two different mechanisms: decreased sensitivity to inhibition by ATP or enhanced channel activation by MgADP.

MATERIALS AND METHODS

Homology modeling

Models of human SUR2A (Fig. 1) were built using Modeller v9.8 from the template of the multidrug ABC transporter Sav1866 (*2ONJ*, to model the "open" conformation) and heterodimeric ABC transporter TM287-TM288 (*3QF4*, to model the "closed" conformation), respectively. The TM0 domain and L0 loop (1–281) were omitted because of lack of sequence homology to any proteins of known structure. Two extended loops unique to SUR2A were also omitted: one connecting TM1 and NBD1 (614–672) and a second connecting NBD1 and TM2 (920–966). A multiple

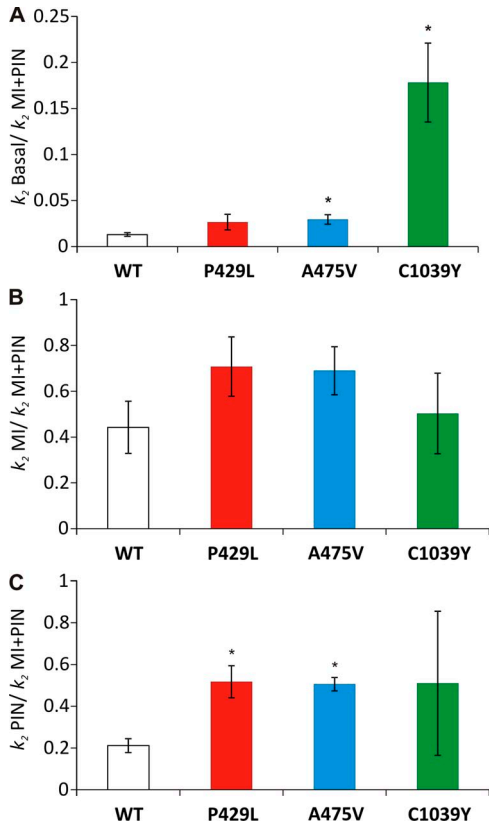

Figure 4. Relative K_{ATP} conductance is markedly increased in basal and stimulated conditions in intact cells expressing homomeric C1039Y K_{ATP} channels. (A–C) The ratio of the rate constants for K_{ATP}-dependent $^{86}Rb^+$ efflux (k_2) in basal and PIN- or MI-stimulated conditions to the maximal activation (in MI+PIN) is plotted for WT and mutant channels. *, $P < 0.05$ as compared with WT (unpaired Student's *t* test). Error bars represent mean ± SEM.

TABLE 1
Rate constants for homomeric fluxes

Condition	Mean	SEM	*n*
Basal			
k_1			
GFP	0.017	0.001	11
k_2			
SUR2A-WT	0.001	0.000	11
P429L	0.004	0.001	8
A475V	0.004	0.001	8
C1039Y	0.003	0.001	8
k_{-1}			
GFP	0.029	0.001	
k_{-2}			
	0.000	0.000	
MI			
k_1			
GFP	0.026	0.005	9
k_2			
SUR2A-WT	0.043	0.007	9
P429L	0.089	0.016	6
A475V	0.098	0.014	6
C1039Y	0.015	0.007	7
k_{-1}			
GFP	0.068	0.010	
k_{-2}			
	−0.006	0.006	
PIN			
k_1			
GFP	0.018	0.001	6
k_2			
SUR2A-WT	0.016	0.002	6
P429L	0.052	0.010	4
A475V	0.060	0.005	4
C1039Y	0.005	0.001	4
k_{-1}			
GFP	0.028	0.002	
k_{-2}			
	0.009	0.002	
MI+PIN			
k_1			
GFP	0.016	0.007	6
k_2			
SUR2A-WT	0.101	0.033	7
P429L	0.097	0.024	7
A475V	0.125	0.030	7
C1039Y	0.013	0.007	8
k_{-1}			
GFP	0.029	0.001	
k_{-2}			
	0.074	0.014	

sequence alignment (MSA) was performed using ClustalW2 between SUR2 and the two template sequences in conjunction with other proteins of the human ABCC family (ABCC1, 2, 3, 4, 5, 6, 8, and 10) for TM1 and NBD1 because of low sequence identity. High sequence identity enabled a reliable sequence alignment of TMD2 and NBD2 by MSA between SUR2 and SUR1, 2ONJ, and 3QF4.

ABCC9 mutagenesis and heterologous expression of K_{ATP} channels

The Quick Change II Site-Directed Mutagenesis kit (Agilent Technologies) was used to engineer P429L, A475V, and C1039Y mutations (equivalent to CS-associated P432L, A478V, and C1043Y mutations in human SUR2; Harakalova et al., 2012; van Bon et al., 2012) into rat SUR2A-pCMV6. Mutations were confirmed by direct sequencing of the entire SUR2A coding region. For channel expression, COSm6 cells were cultured in Dulbecco's modified Eagle's medium (DMEM) supplemented with 10% fetal bovine serum, 10^5 U/L penicillin, and 100 mg/L streptomycin. At 60–70% confluence, cells were transfected with the relevant plasmids using FuGENE6 transfection reagent (Promega). For experiments with homomeric CS mutant channels, cells were cotransfected with pCDNA3.1-mKir6.2-WT (0.6 µg) and WT or mutant pCMV6-ratSUR2A (SUR2) (1 µg). For experiments using heteromeric channels, cells were cotransfected with Kir6.2-WT, SUR2-WT, and mutant SUR2 at ratios of 0.6:0.5:0.5 (w/w/w). Cells transfected with GFP-pcDNA3.1 served as controls. A small amount of GFP DNA was coexpressed for identification of transfected cells in electrophysiology experiments.

Macroscopic $^{86}Rb^+$ efflux assays

Cells were incubated overnight at 37°C in DMEM containing 1 µCi/ml ^{86}RbCl (PerkinElmer), and then incubated in Ringer's solution (mM: 118 NaCl, 10 HEPES, 25 $NaHCO_3$, 4.7 KCl, 1.2 KH_2PO_4, 2.5 $CaCl_2$, and 1.2 $MgSO_4$, adjusted to pH 7.4 with NaOH) in (a) the absence (basal) or (b) the presence of 2.5 mg/ml oligomycin and 1 mM 2-deoxy-D-glucose (metabolic inhibition [MI]), (c) the SUR2-specific K^+ channel opener pinacidil (PIN; 250 µM), or (d) a combination of MI and PIN to achieve maximal channel activation. Subsequently, at selected time points (2.5, 5, 7.5, 15, 25, and 40 min) the solution was collected and replaced with fresh solution. Upon completion of the assay, cells were lysed with 2% SDS and collected, and radioactivity in these samples was measured by liquid scintillation. $^{86}Rb^+$ efflux is expressed as a fraction of total content. A nonspecific efflux that inactivated with time was assumed to be present in all $^{86}Rb^+$ efflux experiments, and apparent rate constants for the K_{ATP}-independent $^{86}Rb^+$ efflux were obtained from GFP-transfected cells using the equation:

$$\text{Rb efflux} = 1 - exp^{-k_1 * e^{(-k_{-1} * t)} \cdot t}, \quad (1)$$

where k_1 and k_{-1} are the apparent activation and inactivation rate constants. K_{ATP}-dependent $^{86}Rb^+$ efflux was also assumed to

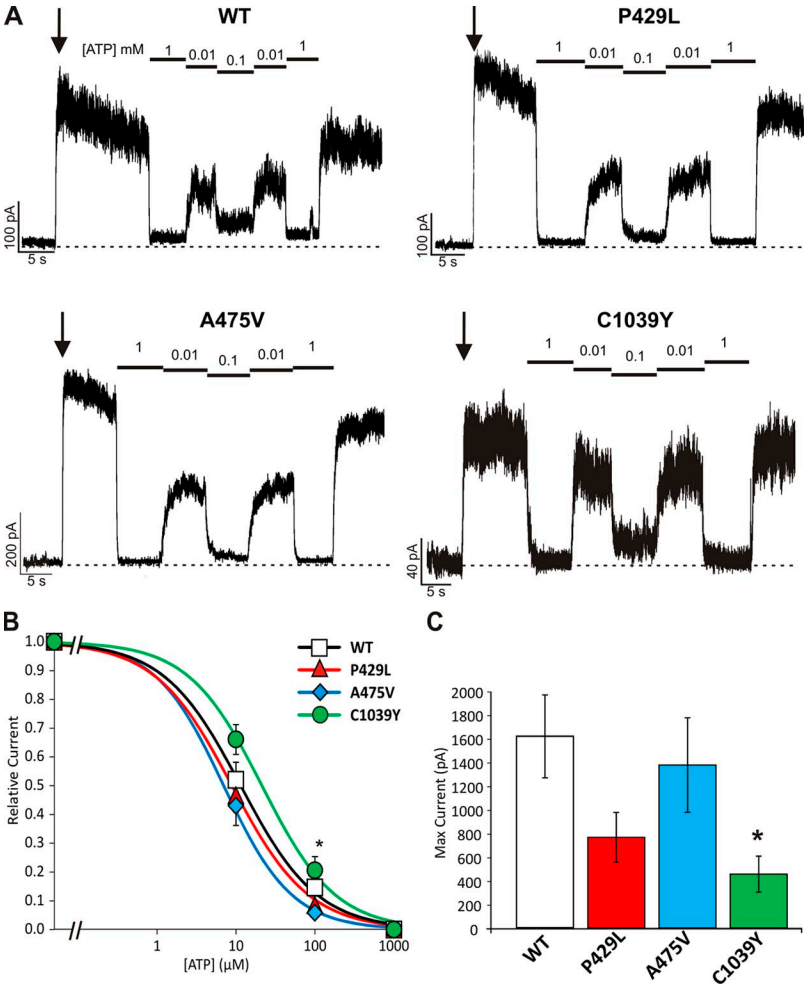

Figure 5. ATP sensitivity is decreased in C1039Y channels. Representative excised patch-current recordings from COSm6 cells coexpressing Kir6.2 and WT or CS mutant SUR2 subunits P429L, A475V, or C1039Y (A). Membrane potential was held at −50 mV, and negative currents (plotted as upward deflections) were recorded continuously on-cell and in inside-out excised patches exposed to K_{INT} in the absence or presence of 0.01, 0.1, or 1 mM ATP; arrowheads mark the point of excision. (B) Dose–response data (mean ± SEM from 8–11 patches) was fit with Eq. 3 to estimate the ATP concentration for half-maximal inhibition K_i: WT (9 µM), P429L (9 µM), A475V (7 µM), and C1039Y (21 µM). (C) Maximum patch-current immediately after patch excision (mean ± SEM from 8–11 patches). *, $P < 0.05$ as compared with WT (unpaired t test). Error bars represent mean ± SEM.

activate and inactivate with time and was obtained using the equation:

$$\text{Rb efflux} = 1 - exp^{-\left(k_1 * e^{(-k_{-1} * t)} + k_2 * e^{(-k_{-2} * t)} \cdot t\right)}, \quad (2)$$

where k_1 and k_{-1} are the rate constants for K_{ATP}-independent pathways (obtained from GFP-transfected cells by Eq. 1), and k_2 and k_{-2} are the activation (k_2) and inactivation (k_{-2}) rate constants for K_{ATP}-specific K^+ conductance. k_2 is then assumed to be proportional to the number of active channels. To account for potential day-to-day variability, for every efflux experiment, a k_1 value was determined for untransfected cells and then incorporated as a fixed parameter in the equation to estimate the K_{ATP}-dependent k_2 for each construct. All k values are listed in Tables 1–3.

Excised patch clamp

After 24–48 h, transfected cells that fluoresced green under UV light were selected for analysis by excised patch-clamp experiments at room temperature in a perfusion chamber that allowed for the rapid switching of solutions. K_{int} solution (mM: 140 KCl, 10 HEPES, and 1 EGTA, pH 7.4) was used as the standard pipette (extracellular) and bath (cytoplasmic) solution in these experiments. ATP or ADP was added as indicated. The appropriate amounts of $MgCl_2$ to be added in each Mg^{2+}-nucleotide–containing solution to attain 0.5 mM of free Mg^{2+} were calculated by means of the CaBuf program (Katholieke Universiteit Leuven). Membrane patches were voltage clamped using an Axopatch 1D amplifier (Molecular Devices), and currents were recorded at −50 mV (pipette voltage, 50 mV) in on-cell and inside-out excised patch configuration. Data were typically filtered at 1 kHz and digitized at 5 kHz with a Digidata 1322A (Molecular Devices) A-D converter. pClamp and Axoscope software (Molecular Devices)

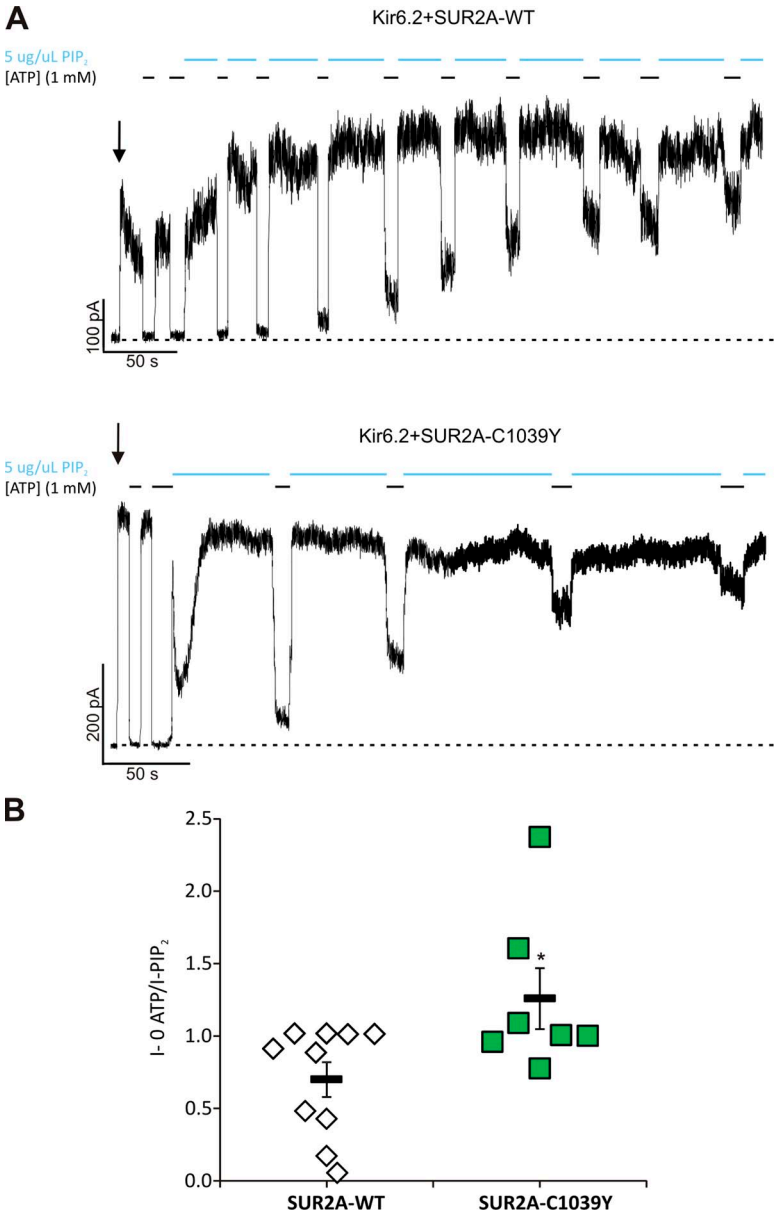

Figure 6. C1039Y channels decreased ATP sensitivity caused by increased P_o. (A) Representative K_{ATP} current traces after excision and in the presence of 1 mM ATP or 5 µg/µl PIP_2 as indicated. (B) Relative P_o determined as a ratio of the maximum steady-state current in the patch upon excision, in the absence of nucleotides over the maximum current measured in PIP_2. Individual patch data are represented by symbols (n = 7–10); error bars are the means ± SEM, respectively relative to P_o = 0.70 ± 0.11 (WT) and 1.26 ± 0.21 (C1039Y). *, $P < 0.05$ as compared with WT (unpaired Student's t test).

were used for data acquisition. For ATP inhibition, [ATP]-response relationships (Fig. 4) were fitted by Eq. 3:

$$I_{rel} = \left\{1 + \left(\frac{[ATP]}{K_i}\right)^H\right\}^{-1}, \quad (3)$$

where I_{rel} (relative current) is the current in the presence of a given concentration of ATP relative to current in zero ATP, K_i is the apparent ATP inhibition constant, and H is the Hill coefficient.

For phosphatidylinositol (4,5)-bisphosphate (PIP_2) activation experiments, an ammonium salt of L-α-phosphatidylinositol-4,5-bisphosphate from porcine brain (Brain PI(4,5)P2; Avanti Polar Lipids, Inc.) was dissolved in K_{INT} to make a 5-μg/μl working solution. For each patch, we estimated the relative P_o by dividing the maximum steady-state current in zero ATP by the maximum steady-state current in PIP_2.

RESULTS

Homomeric mutant channels are overactive in various metabolic conditions

CS-associated mutations have been found throughout the coding sequence (Fig. 1). For the present study, we focused on two previously unexamined mutations (human A478V and C1043Y corresponding to rat A475V and C1039Y, respectively), located in the TMD1 and TMD2 segments, and P432L (corresponding to rat P429L), also located in the TMD1 region. To examine K_{ATP} channel activity in intact cells, we performed $^{86}Rb^+$ efflux assays under four different conditions: basal, MI, in the presence of PIN, and MI and PIN combined (MI+PIN). As shown in Figs. 2 and 3, homomeric expression of SUR2A-P429L, A475V, or C1039Y channels, results in a significantly higher basal $^{86}Rb^+$ efflux rate compared with WT (Figs. 2 A and 3 A). P429L- and A475V-based channels, but not those composed of C1039Y, also showed a significantly higher rate of efflux compared with WT channels under MI conditions and in the presence of PIN (Figs. 2, B and C, and 3, B and C), consistent with the GOF observed in the basal condition. Maximal efflux rates (estimated using simultaneous exposure to MI and PIN) of P429L and A475V were comparable to SUR2A-WT, implying similar channel densities at the cell surface (Figs. 2 D and 3 D). C1039Y showed significantly lower absolute fluxes in all stimulatory conditions (Figs. 2, B–D, and 3, B–D), implying a lower channel density at the membrane (Fig. 4).

The ratio of K_{ATP}-dependent (k_2) rate constants in basal, MI, and PIN to the maximal K_{ATP}-dependent rate

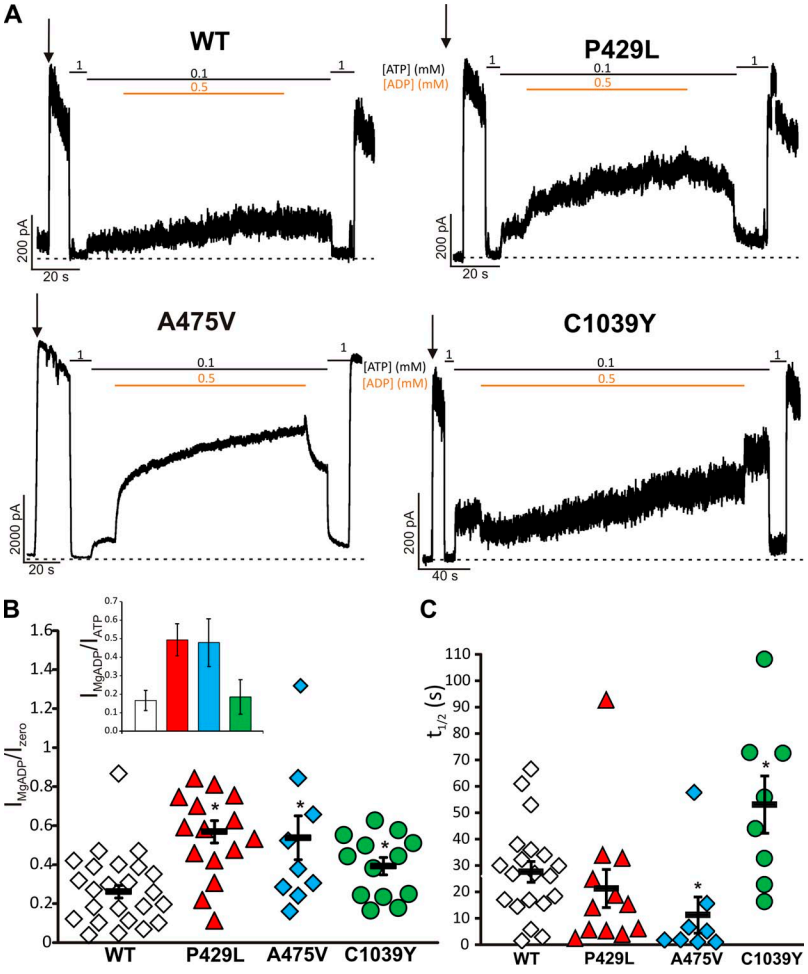

Figure 7. P429L and A475V show enhanced MgADP activation. (A) Representative K_{ATP} current traces after excision and in the presence of nucleotides as indicated. (B) MgADP activation, as a ratio between the steady-state current in the presence of MgADP and the maximum current measured in the patch upon excision, in the absence of nucleotides. Individual patch data represented by symbols (n = 11–24); error bars are the means ± SEM, respectively 26.8 ± 0.03% (WT), 56.9 ± 0.06% (P429L), 59.7 ± 0.1% (A475V), and 38.7 ± 0.04% (C1039Y). *, $P < 0.05$ as compared with WT (unpaired Student's t test). Inset shows the mean current measured in patches in the presence of 0.1 mM of Mg-free ATP (from Fig. 5 B) subtracted from the mean value of steady-state current measured in patches in the presence of MgADP (from Fig. 7 A). Error bars represent the propagated error from both experiments. (C) Half-time of activation by MgADP.

constant (in MI+PIN) should reflect the relative activation of each channel in these specific conditions. In the basal condition, the ratio was higher for all three mutations than for WT, markedly so for C1039Y (Fig. 4 A). In PIN alone, although only P429L and A475V reach significance, the ratio of active channels in all three mutations are also increased (Fig. 4 C). Collectively, the results suggest that each mutant will result in higher channel activation under any stimulatory conditions, particularly for C1039Y.

TABLE 2
Rate constants for heteromeric fluxes

Condition	Mean	SEM	*n*
Basal			
k_1			
GFP	0.019	0.001	8
k_2			
SUR2A-WT	0.001	0.000	8
P429L	0.001	0.000	3
A475V	0.001	0.001	3
C1039Y	0.001	0.000	3
k_{-1}			
GFP	0.029	0.001	
k_{-2}			
	0.000	0.000	
MI			
k_1			
GFP	0.027	0.005	8
k_2			
SUR2A-WT	0.044	0.007	8
P429L	0.040	0.009	3
A475V	0.047	0.010	3
C1039Y	0.017	0.003	3
k_{-1}			
GFP	0.068	0.010	
k_{-2}			
	−0.006	0.006	
PIN			
k_1			
GFP	0.018	0.002	5
k_2			
SUR2A-WT	0.017	0.002	5
P429L	0.022	0.004	4
A475V	0.026	0.005	4
C1039Y	0.007	0.000	4
k_{-1}			
GFP	0.028	0.002	
k_{-2}			
	0.009	0.002	
MI+PIN			
k_1			
GFP	0.019	0.003	4
k_2			
SUR2A-WT	0.091	0.004	4
P429L	0.077	0.002	3
A475V	0.096	0.007	3
C1039Y	0.047	0.002	4
k_{-1}			
GFP	0.029	0.001	
k_{-2}			
	0.074	0.014	

C1039Y (hC1043Y) overactivity results from enhanced open-state stability and decreased ATP sensitivity

$^{86}Rb^+$ flux assays provide evidence for overactivity in CS mutants, but do not provide any indication of underlying molecular mechanisms. We assessed the details of channel properties in inside-out excised patch-clamp electrophysiology experiments. Intrinsic sensitivity to ATP inhibition (in zero Mg^{2+}) was similar for WT, P429L, and A475V channels (K_i = 7–9 µM). However, K_{ATP} channels expressing C1039Y exhibited a significant right shift in ATP sensitivity (K_i = 21.3 µM; Fig. 5 B). A diminished sensitivity to intracellular ATP may account, at least in part, for the increased activity of C1039Y-based K_{ATP} channels in basal conditions in the intact cell (Figs. 2 A and 3 A). Consistent with reduced channel density, the maximal current in zero ATP was significantly lower in C1039Y channels than in WT, P429L, or A475V channels (Fig. 5 C). The P_o in the absence of inhibitory ATP (zero) was estimated by the application of PIP_2 (Koster et al., 2005). After the application of PIP_2, both WT and C1039Y channels lost ATP sensitivity; however, the current in zero ATP increased for WT channels but not for C1039Y channels (Fig. 6). The ratio of the initial maximum current in zero ATP to that in PIP_2 (WT: 0.70 ± 0.11 vs. C1039Y: 1.26 ± 0.21) reflects marked increase in WT maximum P_o but no increase for C1039Y.

Overactivity in P429L (hP432L) and A475V (hA478V) results from increased MgADP activation

We investigated the current response to intracellular MgADP in the presence of 0.1 mM ATP (Fig. 7 A). MgADP-dependent activation was estimated as the ratio between the steady-state activated current in MgADP+ATP and the maximal current in zero ATP, immediately after excision (Fig. 7 B). The relative current in MgADP was markedly higher than WT for P429L and A475V channels. Using this analysis, the current was also statistically higher for C1039Y channels. However, this analysis ignores the intrinsically lower sensitivity of C1039Y channels to ATP inhibition (Fig. 5 C). An alternative estimation for the stimulatory action of Mg nucleotides is to calculate the ratio of current in MgADP+ATP to that in Mg-free ATP alone (Fig. 7 B, inset). This analysis implies no difference in the MgADP activation of C1039Y and WT channels. In addition, although the MgADP activation for P429L and A475V channels is more rapid than WT, activation of the C1039Y channel is even slower than WT (Fig. 7 C).

GOF is reduced in heteromeric mutant channels

All documented CS patients with mutations in *ABCC9* are heterozygous. To mimic the predicted heteromeric composition of channels in such patients, we also expressed each mutation in a 1:1 ratio with SUR2A-WT plus Kir6.2, and assessed channel activity by $^{86}Rb^+$ efflux assays (Figs. 8 and 9). In all conditions, P429L, A475V, and C1039Y heteromeric channels display no significant increases in the rate of $^{86}Rb^+$ efflux compared with WT channels (Figs. 8 A and 9 A). When normalized to the maximal efflux rates, channels with heteromeric expression of C1039Y are still considerably less active than WT. In the heteromeric state, maximal C1039Y channel fluxes were markedly higher than in the homomeric state (Fig. 9 D), also implying a partial rescue of the surface expression of C1039Y subunits by WT subunits (Figs. 8, B–D, and 9, B–D).

Altered response to glibenclamide in C1039Y channels

Some NDM patients with GOF mutations in Kir6.2 or SUR1 have successfully been switched from insulin therapy to K_{ATP} inhibitors such as glibenclamide (Zung et al., 2004). However, a correlation between increased channel activity and diminished effectiveness of such drugs has been noted (Koster et al., 2005). Therefore, to test the effectiveness of glibenclamide on overactive P429L, A475V, or C1039Y channels, expressed both homomerically and heteromerically; $^{86}Rb^+$ efflux experiments were performed in the presence of MI plus 10 µM glibenclamide (Fig. 10). The time course of Rb^+ effluxes

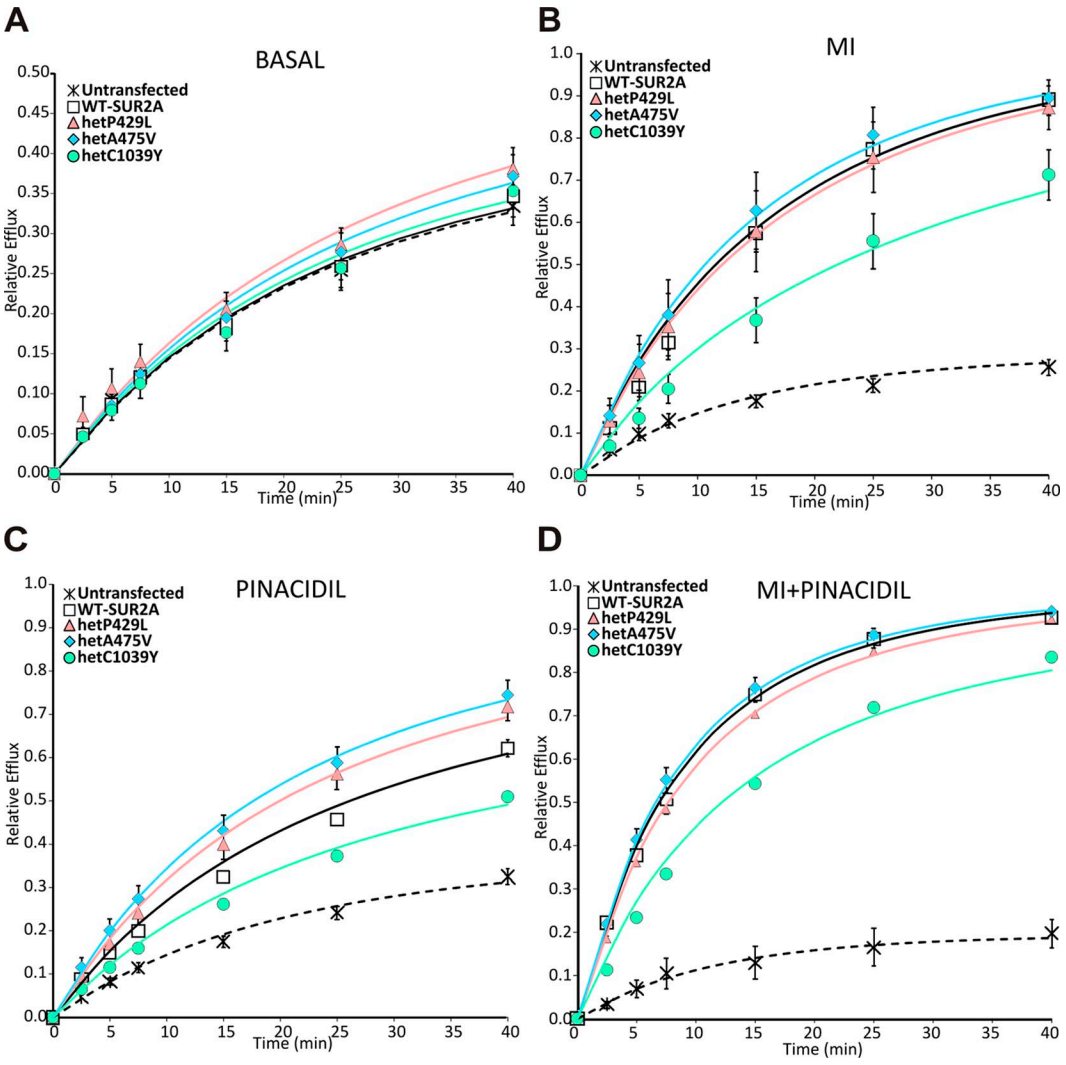

Figure 8. Channel activity in cells expressing heteromeric P429L-, A475V-, or C1039Y-based K_{ATP} channels. $^{86}Rb^+$ efflux as a function of time was measured in GFP-transfected control cells (dashed) and in cells transiently expressing reconstituted Kir6.2-based K_{ATP} channels with WT or 1:1 mixtures of WT and P429L, A475V, or C1039Y mutant SUR2 subunits in basal conditions (A), in the presence of MIs oligomycin and 2-deoxy-D-glucose (B), in the K^+ channel opener PIN (C), or in the presence of both MI and PIN (D). The data represent means ± SEM of 6–10 experiments. Flux data were fit with Eq. 1 (GFP) to obtain the rate constant k_1 or Eq. 2 to obtain the rate constants for K_{ATP}-dependent efflux, k_2 (Fig. 3), where lines show mean fitted relationships.

shows an unusual behavior in that although initial fluxes are markedly lower than in MI alone, the inhibition is not maintained through the time course of the assay. It is well understood that the inhibitory action of glibenclamide is a complex function of the metabolic conditions and decreases under conditions of MI (Findlay, 1994; Koster et al., 1999). To account for this behavior, the efflux data in glibenclamide were fit by Eq. 2, where positive values for k_{-2} now result in the rate of efflux actually increasing with time for A475V and P429L channels (see Table 3). From this analysis, the ratio of the k_2 in MI plus glibenclamide to k_2 in MI provides an estimate of the relative sensitivity to inhibition by glibenclamide (Fig. 10 C). Although the glibenclamide sensitivity of A475V and P429L channels was not different from WT, C1039Y channels appeared almost insensitive to the drug. Qualitatively similar results were obtained with channels expressed in heteromeric mixture with WT subunits (Fig. 10, B–D). As discussed below, this glibenclamide insensitivity is consistent with similar findings for SUR1 mutations that produce increased activity of resultant K_{ATP} channels.

DISCUSSION

Distinct mechanisms of K_{ATP} GOF in CS ABCC9 mutations

CS is a rare disease characterized by complex vascular and skeletal anomalies, the underlying cellular and molecular mechanisms of which we are only now beginning to understand (Nichols et al., 2013). The majority of genotyped CS patients are heterozygous for mutations in the genes encoding *ABCC9* (SUR2) (Harakalova et al., 2012; van Bon et al., 2012) in most cases, and *KCNJ8* (Kir6.1) (Brownstein et al., 2013; Cooper et al., 2014) in others. A select few of these mutations have thus far been shown to form overactive K_{ATP} channels (Harakalova et al., 2012; Cooper et al., 2014), and most remain unexplored. Here, we characterized three CS-associated *ABCC9* mutations, namely P429L (hP432L), A475V (hA478V), and C1039Y (hC1043Y), that localize

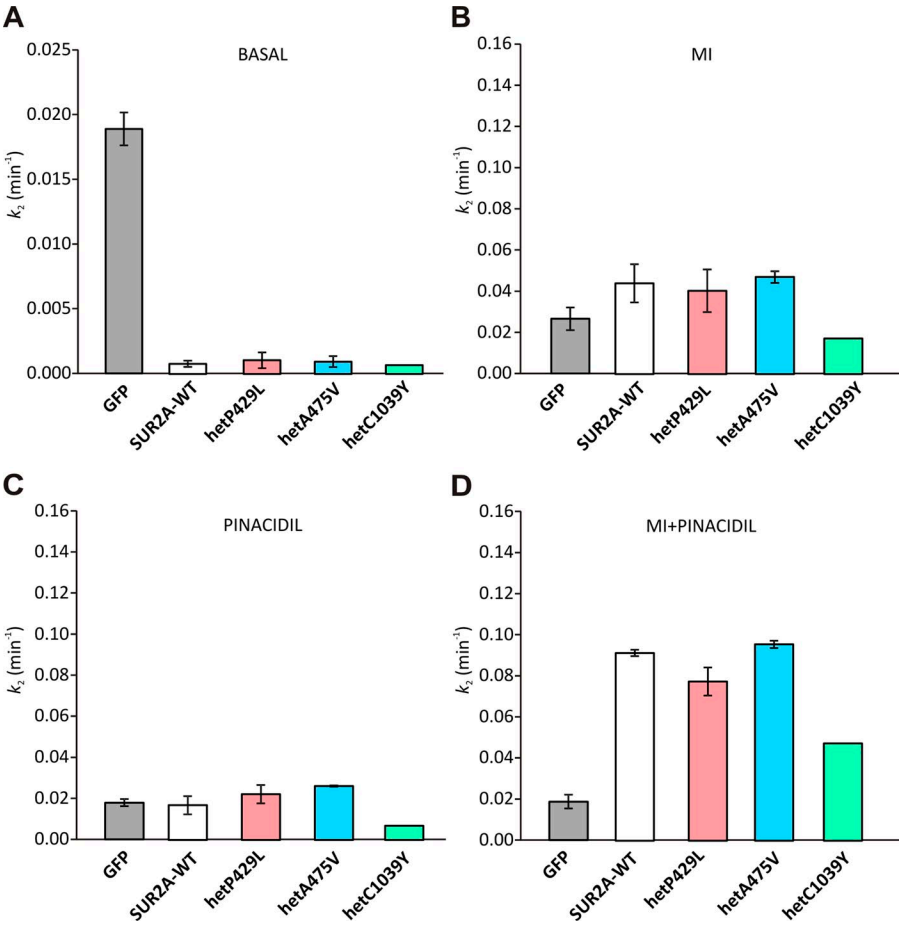

Figure 9. K_{ATP} conductance normalized in basal and stimulated conditions in heteromeric P429L-, A475V-, or C1039Y-based K_{ATP} channels. (A–D) The rate constants for nonspecific efflux (k_1 represented by gray area) and K_{ATP}-dependent $^{86}Rb^+$ efflux (k_2), proportional to K_{ATP}-specific K^+ conductance, were estimated from data shown in Fig. 7. Error bars represent mean ± SEM.

TABLE 3

Rate constants for fluxes in MI+GLIB

Condition	Mean	SEM	*n*
MI+GLIB			
k_1			
GFP	0.020	0.004	7
k_2			
SUR2A-WT	0.004	0.001	7
P429L	0.005	0.003	4
A475V	0.005	0.001	6
C1039Y	0.007	0.002	6
hetP429L	0.003	0.001	3
hetA475V	0.005	0.000	3
hetC1039Y	0.004	0.001	3
MI+GLIB			
k_{-1}			
GFP	0.053	0.009	7
k_{-2}			
SUR2A-WT	−0.047	0.008	7
P429L	−0.039	0.028	4
A475V	−0.045	0.010	4
C1039Y	−0.003	0.013	6
hetP429L	−0.030	0.010	3
hetA475V	−0.042	0.006	3
hetC1039Y	−0.031	0.010	3

MI+GLIB, MI plus glibenclamide.

to distinct regions of the SUR2 protein (Fig. 1). Each mutation leads to K_{ATP} channel GOF (Figs. 2–7), consistent with previous findings on isolated CS-associated *ABCC9* mutations (Harakalova et al., 2012).

In the only previous assessment of CS-associated *ABCC9* mutations, Harakalova et al. (2012) measured channel sensitivity to ATP in the presence of Mg^{2+}. Mg nucleotides have complex activatory/inhibitory effects on K_{ATP} channels: MgATP can both inhibit the Kir6.X subunit and be hydrolyzed to activatory MgADP at the SUR subunits (Nichols, 2006). Therefore, such an analysis cannot separate mutant effects on ATP inhibition from those on Mg nucleotide activation. By separately assessing channel activity in response to Mg-free ATP and to MgADP, we show that CS-associated *ABCC9* mutations lead to increased channel activity via different mechanisms, as has also been observed with NDM-associated *ABCC8* mutations (de Wet et al., 2007a, 2008; Masia et al., 2007; Zhou et al., 2010). Specifically, we demonstrate that increased activity of P429L and A475V channels results from increased MgADP activation, whereas increased activity of C1039Y channels results predominantly from decreased ATP sensitivity caused by higher intrinsic open-state stability.

Some NDM-causing GOF mutations in SUR1 have also been shown to reduce ATP sensitivity (Tarasov et al., 2008; Takagi et al., 2013), either by reducing inhibitory ATP-binding affinity or by increasing the intrinsic open-state stability of the channel (Shyng and Nichols, 1998; Koster et al., 2005). That PIP_2 decreases ATP sensitivity, but does not increase maximum currents, in the C1039Y channel implies that the intrinsic P_o of these channels is near 1 (relative P_o = 1.26 ± 0.21), significantly higher than for WT channels (relative P_o = 0.70 ± 0.11; Fig. 6), explaining the intrinsically lower ATP sensitivity of the C1039Y channel.

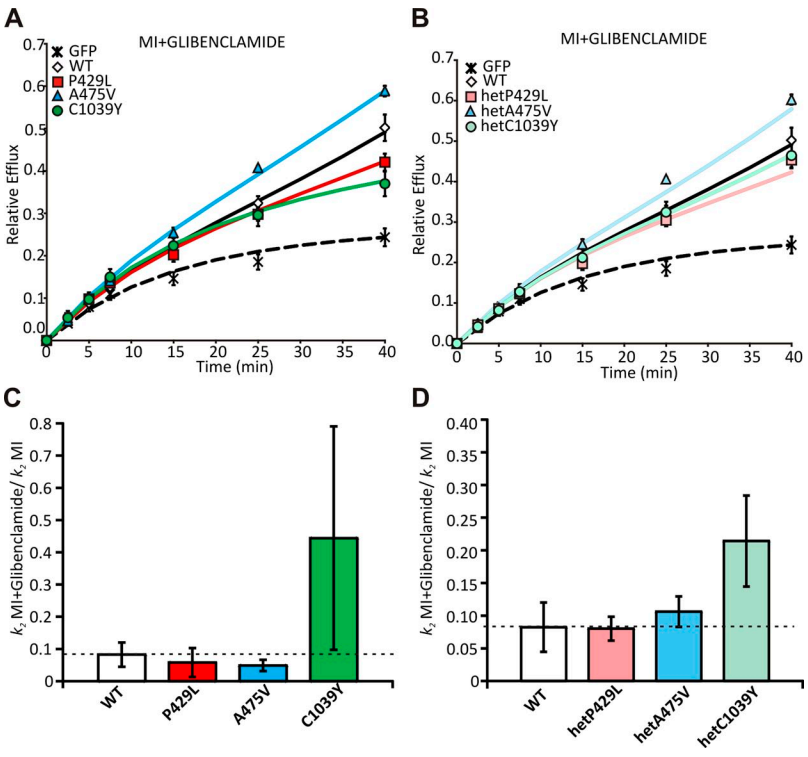

Figure 10. Decreased sensitivity to glibenclamide inhibition in C1039Y channels. $^{86}Rb^+$ efflux as a function of time was measured in GFP-transfected control cells and in cells transiently expressing K_{ATP} channels composed of Kir6.2 plus WT or mutant SUR2 subunits (A), as well as in cells expressing a 1:1 mixture of WT and mutant SUR2 subunits. (B) Experiments were performed in MI plus glibenclamide. The data represent the means ± SEM of three to six experiments. Data were fit with Eq. 2 to obtain rate constants for K_{ATP}-dependent efflux, k_2. (C and D) k_2 in glibenclamide plus MI divided by k_2 in MI for each condition.

In addition to increasing channel activity, homomeric expression of C1039Y appears to decrease expression of channels in the membrane, detectable in both $^{86}Rb^+$ flux and patch-clamp analyses. A similar dual effect of GOF mutations in both Kir6.2 (Lin et al., 2013) and SUR1 (Zhou et al., 2010) has been shown previously. In these previous examples, decreased surface expression was demonstrated by Western blot analysis. Significant rescue of channel activity in heteromeric C1039Y/WT channels is consistent with the patterns from such mutations (Figs. 8 and 9); therefore, we suggest that in addition to reducing ATP sensitivity of expressed channels, C1039Y also decreases K_{ATP} surface expression.

Implications for tissue pathology in CS

Kir6.1 GOF mutations have also been found in two CS patients (Brownstein et al., 2013; Cooper et al., 2014), confirming Kir6.1/SUR2 as the key subunit combination generating the overactive channels. Given the experimental difficulty of recording Kir6.1/SUR2 currents (Cooper et al., 2014), we used Kir6.2+SUR2A channels in the present study. *ABCC9* encodes two splice variants: SUR2A and SUR2B, which vary only in the last 40 amino acids. All CS-associated SUR2 mutations identified thus far are found within the core of the SUR2 protein, such that these mutations will be present in both SUR2A and SUR2B. SUR2A is predominant in skeletal muscle and heart, whereas SUR2B is expressed in the vasculature. 6.1/SUR2B may be the more dramatically affected combination, as vascular phenotypes seem to predominate in CS patients (Nichols et al., 2013): neither skeletal muscle weakness nor shortening of the QT interval on the electrocardiogram has been noted, as might be expected if Kir6.2/SUR2A were markedly activated.

The severity of disease varies between CS patients such that not all reported features are exhibited by all patients. Direct comparison of the phenotypes of patients carrying the A475V and C1039Y equivalent mutations (van Bon et al., 2012) revealed hypertrichosis, macrosomia, macrocephaly, coarse features, cardiac anomalies, and umbilical hernia to be common to both, but pulmonary hypertension, cardiomegaly, osteopenia, hyperextensibility and lymphedema were only reported for the A475V equivalent patient. Because the reduced sensitivity to ATP inhibition caused by the C1039Y mutation results in greater relative basal channel activity than does the enhanced Mg nucleotide activation caused by A475V, a less severe disease phenotype for C1039Y suggests that reduced expression caused by this mutation may also be a consequence in vivo, as also reported for SUR1 NDM mutations (Zhou et al., 2010).

Implications for therapeutic intervention in CS

Finally, sulfonylureas, which inhibit K_{ATP} channels via interaction with the SUR subunits, are effective treatments for NDM patients with *ABCC8*-activating mutations (Babenko et al., 2006), and may be promising potential therapies for CS (Nichols et al., 2013). However, GOF mutations in Kir6.2 (Koster et al., 2005) and SUR1 (Takagi et al., 2013) that increase channel open-state stability also typically decrease sensitivity to sulfonylureas, which may result in a lack of sulfonylurea therapeutic efficacy in patients with these mutations. Assessment of $^{86}Rb^+$ efflux in glibenclamide (Fig. 10) suggests that the same can be true of SUR2 GOF mutations, specifically C1039Y channels, which required a significantly higher k_2 value, indicating reduced glibenclamide sensitivity (see Table 3). However, in general, SUR2 sensitivity to sulfonylureas is much lower than SUR1 sensitivity to these drugs (Dörschner et al., 1999), and so, given the further reduction in drug sensitivity of GOF mutants, the introduction of sulfonylureas to treat CS patients is likely to require high doses, such that undesired inhibition of SUR1-based K_{ATP} channels, leading to hypoglycemic effects, will need to be carefully considered. Such concerns may ultimately necessitate the development of Kir6.1- or SUR2-specific inhibitors to provide safer and more effective treatment options for CS patients.

This work was supported by National Institutes of Health (NIH) grant HL95010 (to C.G. Nichols). P.E. Cooper was supported by NIH training grant HL007275.

The authors declare no competing financial interests.

Merritt C. Maduke served as editor.

Submitted: 10 August 2015
Accepted: 13 October 2015

REFERENCES

Aguilar-Bryan, L., C.G. Nichols, S.W. Wechsler, J.P. Clement IV, A.E. Boyd III, G. González, H. Herrera-Sosa, K. Nguy, J. Bryan, and D.A. Nelson. 1995. Cloning of the beta cell high-affinity sulfonylurea receptor: a regulator of insulin secretion. *Science.* 268:423–426. http://dx.doi.org/10.1126/science.7716547

Akrouh, A., S.E. Halcomb, C.G. Nichols, and M. Sala-Rabanal. 2009. Molecular biology of K(ATP) channels and implications for health and disease. *IUBMB Life.* 61:971–978. http://dx.doi.org/10.1002/iub.246

Ashford, M.L., N.C. Sturgess, N.J. Trout, N.J. Gardner, and C.N. Hales. 1988. Adenosine-5′-triphosphate-sensitive ion channels in neonatal rat cultured central neurones. *Pflugers Arch.* 412:297–304. http://dx.doi.org/10.1007/BF00582512

Babenko, A.P., M. Polak, H. Cavé, K. Busiah, P. Czernichow, R. Scharfmann, J. Bryan, L. Aguilar-Bryan, M. Vaxillaire, and P. Froguel. 2006. Activating mutations in the ABCC8 gene in neonatal diabetes mellitus. *N. Engl. J. Med.* 355:456–466. http://dx.doi.org/10.1056/NEJMoa055068

Brownstein, C.A., M.C. Towne, L.J. Luquette, D.J. Harris, N.S. Marinakis, P. Meinecke, K. Kutsche, P.M. Campeau, T.W. Yu, D.M. Margulies, et al. 2013. Mutation of KCNJ8 in a patient with Cantú syndrome with unique vascular abnormalities—Support for the role of K(ATP) channels in this condition. *Eur. J. Med. Genet.* 56:678–682. http://dx.doi.org/10.1016/j.ejmg.2013.09.009

Cantú, J.M., D. García-Cruz, J. Sánchez-Corona, A. Hernández, and Z. Nazará. 1982. A distinct osteochondrodysplasia with hypertrichosis—Individualization of a probable autosomal recessive

entity. *Hum. Genet.* 60:36–41. http://dx.doi.org/10.1007/BF00281261

Cook, D.L., and C.N. Hales. 1984. Intracellular ATP directly blocks K^+ channels in pancreatic B-cells. *Nature.* 311:271–273. http://dx.doi.org/10.1038/311271a0

Cooper, P.E., H. Reutter, J. Woelfle, H. Engels, D.K. Grange, G. van Haaften, B.W. van Bon, A. Hoischen, and C.G. Nichols. 2014. Cantú syndrome resulting from activating mutation in the KCNJ8 gene. *Hum. Mutat.* 35:809–813. http://dx.doi.org/10.1002/humu.22555

de Wet, H., M.V. Mikhailov, C. Fotinou, M. Dreger, T.J. Craig, C. Vénien-Bryan, and F.M. Ashcroft. 2007a. Studies of the ATPase activity of the ABC protein SUR1. *FEBS J.* 274:3532–3544. http://dx.doi.org/10.1111/j.1742-4658.2007.05879.x

de Wet, H., M.G. Rees, K. Shimomura, J. Aittoniemi, A.M. Patch, S.E. Flanagan, S. Ellard, A.T. Hattersley, M.S. Sansom, and F.M. Ashcroft. 2007b. Increased ATPase activity produced by mutations at arginine-1380 in nucleotide-binding domain 2 of ABCC8 causes neonatal diabetes. *Proc. Natl. Acad. Sci. USA.* 104:18988–18992. http://dx.doi.org/10.1073/pnas.0707428104

de Wet, H., P. Proks, M. Lafond, J. Aittoniemi, M.S. Sansom, S.E. Flanagan, E.R. Pearson, A.T. Hattersley, and F.M. Ashcroft. 2008. A mutation (R826W) in nucleotide-binding domain 1 of ABCC8 reduces ATPase activity and causes transient neonatal diabetes. *EMBO Rep.* 9:648–654. http://dx.doi.org/10.1038/embor.2008.71

Dörschner, H., E. Brekardin, I. Uhde, C. Schwanstecher, and M. Schwanstecher. 1999. Stoichiometry of sulfonylurea-induced ATP-sensitive potassium channel closure. *Mol. Pharmacol.* 55:1060–1066.

Findlay, I. 1994. The ATP sensitive potassium channel of cardiac muscle and action potential shortening during metabolic stress. *Cardiovasc. Res.* 28:760–761. http://dx.doi.org/10.1093/cvr/28.6.760

Gloyn, A.L., E.R. Pearson, J.F. Antcliff, P. Proks, G.J. Bruining, A.S. Slingerland, N. Howard, S. Srinivasan, J.M. Silva, J. Molnes, et al. 2004. Activating mutations in the gene encoding the ATP-sensitive potassium-channel subunit Kir6.2 and permanent neonatal diabetes. *N. Engl. J. Med.* 350:1838–1849. http://dx.doi.org/10.1056/NEJMoa032922

Harakalova, M., J.J. van Harssel, P.A. Terhal, S. van Lieshout, K. Duran, I. Renkens, D.J. Amor, L.C. Wilson, E.P. Kirk, C.L. Turner, et al. 2012. Dominant missense mutations in ABCC9 cause Cantú syndrome. *Nat. Genet.* 44:793–796. http://dx.doi.org/10.1038/ng.2324

Inagaki, N., T. Gonoi, J.P. Clement IV, N. Namba, J. Inazawa, G. Gonzalez, L. Aguilar-Bryan, S. Seino, and J. Bryan. 1995a. Reconstitution of I_{KATP}: An inward rectifier subunit plus the sulfonylurea receptor. *Science.* 270:1166–1170. http://dx.doi.org/10.1126/science.270.5239.1166

Inagaki, N., Y. Tsuura, N. Namba, K. Masuda, T. Gonoi, M. Horie, Y. Seino, M. Mizuta, and S. Seino. 1995b. Cloning and functional characterization of a novel ATP-sensitive potassium channel ubiquitously expressed in rat tissues, including pancreatic islets, pituitary, skeletal muscle, and heart. *J. Biol. Chem.* 270:5691–5694. http://dx.doi.org/10.1074/jbc.270.11.5691

Inagaki, N., T. Gonoi, J.P. Clement, C.Z. Wang, L. Aguilar-Bryan, J. Bryan, and S. Seino. 1996. A family of sulfonylurea receptors determines the pharmacological properties of ATP-sensitive K^+ channels. *Neuron.* 16:1011–1017. http://dx.doi.org/10.1016/S0896-6273(00)80124-5

Koster, J.C., Q. Sha, and C.G. Nichols. 1999. Sulfonylurea and K^+-channel opener sensitivity of K_{ATP} channels. Functional coupling of Kir6.2 and SUR1 subunits. *J. Gen. Physiol.* 114:203–213. http://dx.doi.org/10.1085/jgp.114.2.203

Koster, J.C., M.S. Remedi, C. Dao, and C.G. Nichols. 2005. ATP and sulfonylurea sensitivity of mutant ATP-sensitive K^+ channels in neonatal diabetes: Implications for pharmacogenomic therapy. *Diabetes.* 54:2645–2654. http://dx.doi.org/10.2337/diabetes.54.9.2645

Lin, Y.W., A. Li, V. Grasso, D. Battaglia, A. Crinò, C. Colombo, F. Barbetti, and C.G. Nichols. 2013. Functional characterization of a novel *KCNJ11* in frame mutation-deletion associated with infancy-onset diabetes and a mild form of intermediate DEND: A battle between K_{ATP} gain of channel activity and loss of channel expression. *PLoS One.* 8:e63758. http://dx.doi.org/10.1371/journal.pone.0063758

Masia, R., D. Enkvetchakul, and C.G. Nichols. 2005. Differential nucleotide regulation of KATP channels by SUR1 and SUR2A. *J. Mol. Cell. Cardiol.* 39:491–501. http://dx.doi.org/10.1016/j.yjmcc.2005.03.009

Masia, R., D.D. De Leon, C. MacMullen, H. McKnight, C.A. Stanley, and C.G. Nichols. 2007. A mutation in the TMD0-L0 region of sulfonylurea receptor-1 (L225P) causes permanent neonatal diabetes mellitus (PNDM). *Diabetes.* 56:1357–1362. http://dx.doi.org/10.2337/db06-1746

Nichols, C.G. 2006. KATP channels as molecular sensors of cellular metabolism. *Nature.* 440:470–476. http://dx.doi.org/10.1038/nature04711

Nichols, C.G., S.L. Shyng, A. Nestorowicz, B. Glaser, J.P. Clement IV, G. Gonzalez, L. Aguilar-Bryan, M.A. Permutt, and J. Bryan. 1996. Adenosine diphosphate as an intracellular regulator of insulin secretion. *Science.* 272:1785–1787. http://dx.doi.org/10.1126/science.272.5269.1785

Nichols, C.G., G.K. Singh, and D.K. Grange. 2013. K_{ATP} channels and cardiovascular disease: Suddenly a syndrome. *Circ. Res.* 112:1059–1072. http://dx.doi.org/10.1161/CIRCRESAHA.112.300514

Noma, A. 1983. ATP-regulated K^+ channels in cardiac muscle. *Nature.* 305:147–148. http://dx.doi.org/10.1038/305147a0

Proks, P., K. Shimomura, T.J. Craig, C.A. Girard, and F.M. Ashcroft. 2007. Mechanism of action of a sulphonylurea receptor SUR1 mutation (F132L) that causes DEND syndrome. *Hum. Mol. Genet.* 16:2011–2019. http://dx.doi.org/10.1093/hmg/ddm149

Shyng, S., and C.G. Nichols. 1997. Octameric stoichiometry of the KATP channel complex. *J. Gen. Physiol.* 110:655–664. http://dx.doi.org/10.1085/jgp.110.6.655

Shyng, S.L., and C.G. Nichols. 1998. Membrane phospholipid control of nucleotide sensitivity of KATP channels. *Science.* 282:1138–1141. http://dx.doi.org/10.1126/science.282.5391.1138

Standen, N.B., J.M. Quayle, N.W. Davies, J.E. Brayden, Y. Huang, and M.T. Nelson. 1989. Hyperpolarizing vasodilators activate ATP-sensitive K^+ channels in arterial smooth muscle. *Science.* 245:177–180. http://dx.doi.org/10.1126/science.2501869

Takagi, T., H. Furuta, M. Miyawaki, K. Nagashima, T. Shimada, A. Doi, S. Matsuno, D. Tanaka, M. Nishi, H. Sasaki, et al. 2013. Clinical and functional characterization of the Pro1198Leu ABCC8 gene mutation associated with permanent neonatal diabetes mellitus. *J. Diabetes Investig.* 4:269–273. http://dx.doi.org/10.1111/jdi.12049

Tarasov, A.I., T.J. Nicolson, J.P. Riveline, T.K. Taneja, S.A. Baldwin, J.M. Baldwin, G. Charpentier, J.F. Gautier, P. Froguel, M. Vaxillaire, and G.A. Rutter. 2008. A rare mutation in ABCC8/SUR1 leading to altered ATP-sensitive K^+ channel activity and beta-cell glucose sensing is associated with type 2 diabetes in adults. *Diabetes.* 57:1595–1604. http://dx.doi.org/10.2337/db07-1547

Tucker, S.J., F.M. Gribble, C. Zhao, S. Trapp, and F.M. Ashcroft. 1997. Truncation of Kir6.2 produces ATP-sensitive K^+ channels in the absence of the sulphonylurea receptor. *Nature.* 387:179–183. http://dx.doi.org/10.1038/387179a0

van Bon, B.W., C. Gilissen, D.K. Grange, R.C. Hennekam, H. Kayserili, H. Engels, H. Reutter, J.R. Ostergaard, E. Morava, K. Tsiakas, et al. 2012. Cantú syndrome is caused by mutations in ABCC9. *Am. J. Hum. Genet.* 90:1094–1101. http://dx.doi.org/10.1016/j.ajhg.2012.04.014

Winquist, R.J., L.A. Heaney, A.A. Wallace, E.P. Baskin, R.B. Stein, M.L. Garcia, and G.J. Kaczorowski. 1989. Glyburide blocks the relaxation response to BRL 34915 (cromakalim), minoxidil sulfate and diazoxide in vascular smooth muscle. *J. Pharmacol. Exp. Ther.* 248:149–156.

Zhou, Q., I. Garin, L. Castaño, J. Argente, M.T. Muñoz-Calvo, G. Perez de Nanclares, and S.L. Shyng. 2010. Neonatal diabetes caused by mutations in sulfonylurea receptor 1: Interplay between expression and Mg-nucleotide gating defects of ATP-sensitive potassium channels. *J. Clin. Endocrinol. Metab.* 95:E473–E478. http://dx.doi.org/10.1210/jc.2010-1231

Zung, A., B. Glaser, R. Nimri, and Z. Zadik. 2004. Glibenclamide treatment in permanent neonatal diabetes mellitus due to an activating mutation in Kir6.2. *J. Clin. Endocrinol. Metab.* 89:5504–5507. http://dx.doi.org/10.1210/jc.2004-1241